Rare Metal Materials and Engineering
Volume 49, Issue 7, July 2020
Available online at www.rmme.ac.cn

Science Press

Cite this article as: Rare Metal Materials and Engineering, 2020, 49(7): 2289-2298.

ARTICLE

Effects of Strain Rate and Temperature on the Tensile Deformation Behavior of an Extruded Mg-1Y Sheet

Ji Bin[1], Lu Jiawei[1], Yu Yixiang[2], Yin Dongdi[1]

[1] *Key Laboratory of Advanced Technologies of Materials, Ministry of Education, Southwest Jiaotong University, Chengdu 610031, China;*
[2] *Jiangsu LongSun Electrician Electric Co., Ltd, Yangzhou 225800, China*

Abstract: The tensile deformation behavior of an extruded Mg-1Y (wt%) sheet was investigated in the temperature range of 25 (RT) to 300 ºC and at strain rates from 0.001 to 0.1 s^{-1}. The results show that ultimate tensile strength (UTS) decreases by 49.3% from (247.9 ± 5.8) MPa to (125.6+4.7) MPa when temperature increases from RT to 300 ºC at the strain rate of 0.1 s^{-1}. It is interesting to note that the flow behavior of the studied sheet exhibits pronounced strain rate sensitivity even at RT. The UTS at RT decreases by 11.8% as the strain rate decreasing from 0.1 s^{-1} to 0.001 s^{-1}. The flow behavior of the alloy can be described by the Garofalo hyperbolic sine constitutive equation in the temperature range of RT to 250 ºC. The measured stress exponent n is 27.8 ± 8.9, and the activation energy Q is (124.6 ± 6.1) kJ/mol. The Q value implies that deformation is controlled by dislocation climb. At intermediate temperature (150~250 ºC), the sheet exhibits serrated flow behavior, and this phenomenon is pronounced at lower strain rates. Simultaneously, the elongation to failure (EL) decreases anomalously with the increase of the temperature. The above two deformation features are believed to be closely related to the strong interaction between Y solute atoms and dislocations which is known as dynamic strain aging (DSA). The value of strain rate sensitivity (m) increases with the increase of the temperature. The m increasing from 0.068 to 0.11 at 300 ºC indicates that the addition of Y results in the activation of more slip systems. The deformation microstructure observation reveals that twinning is depressed with temperature, which is consistent with the remarkably increased m values. Dynamic recrystallization (DRX) was observed at 300 ºC, and it is promoted with lower strain rate.

Key words: extruded Mg-1Y sheet; tensile deformation; constitutive equation; strain rate sensitivity

To acquire higher fuel efficiency in the transportation sector for environmental protection, quantity demanded of light-weight materials became bigger[1]. Magnesium (Mg) alloys have wide application prospects in the aerospace and automotive industries since Mg is the lightest of all the engineering metals, and having a density of 1.74 g/cm^3 [2]. In addition, Mg alloys have also the high specific strength, good machinability, and high damping capacity[3,4]. Compared with cast Mg alloys, wrought Mg alloys have better mechanical properties[5,6]. However, widespread use of wrought Mg alloys was limited by their poor formability. Firstly, hexagonal close-packed (hcp) crystal structure which possesses a limited number of slip systems[7, 8] repressed formability. Secondly, a strong basal texture of extruded Mg alloys also resulted in poor formability[6].

To improve Mg alloys formability, it is important to catch the point of the deformation behavior under different deformation conditions. Extensive ranges of magnesium alloys, such as AZ31 AZ80, ZE41, have been researched to discuss the effect of temperature and strain-rate on deformation behavior[9-11]. Maksoud et al[10] detected the AZ31 and found that a decrease in the peak stress and an increase in the fraction of dynamically recrystallized grains with the decrease of the strain rate and the increase of temperature.

Received date: July 15, 2019
Foundation item: National Natural Science Foundation of China (51401172); Sichuan Science and Technology Program (2019YJ0238); Fundamental Research Funds for the Central Universities (2682016CX073)
Corresponding author: Yin Dongdi, Ph. D., Associate Professor, School of Materials Science and Engineering, Southwest Jiaotong University, Chengdu 610031, P. R. China, Tel: 0086-28-87634673, E-mail: ahnydd@swjtu.edu.cn

Maksoud regarded deformation temperature as the major factor of dynamic recrystallization (DRX).

Some researchers investigated that addition of RE can improve mechanical properties. Zhang et al[12] found that addition of Y could remarkably change AZ91 microstructure with the formation of two intermetallic phases. Wu et al[13] dramatically raised the ultimate tensile strength of AZ91D alloys by adding Res. Lu et al[14] showed the ultimate tensile strength of WGZ1152 was over 300 MPa at room temperature (RT). Stanford et al[15] increased the ductility of Mg alloys by additions of rare earth elements. Huang et al[6] found that the addition of Y can weaken basal texture and improve strength. However few types of research have been done to investigate the detailed tensile deformation behavior of Mg-Y binary alloys at different temperatures and strain rates.

The aim of this work was to investigate the tensile behavior of an extruded Mg-1Y sheet in the temperature range of 25~300 ºC, and the strain rate range from 0.001 to 0.1 s^{-1}. The effect of temperature and strain rate on stress was discussed. The temperature, strain rate, and peak stress were described by the Garofalo hyperbolic sine constitutive equation in a temperature range of 25 to 250 ºC. The SRS was also discussed and revealed to interpret deformation behavior.

1 Experiment

The material was prepared by melting purity Mg (99.99%) and Mg-30Y master alloy in a steel crucible with a mixed atmosphere of CO_2 and SF_6 (the ratio of CO_2 and SF_6 is 100:1). Then pouring was conducted in a steel mold with gravity and the as-cast ingots' diameters were 95 mm. The as-cast ingots were homogenized at 530 ºC for 8 h, and then were machined into 90 mm diameter size. Sheets with a cross section of 80 mm×5 mm were extruded from the 90 mm diameter casting ingot with an extrusion ratio of 16. The extrusion billets were 300 ºC and the mold was 400 ºC. The actual composition of the studied material was Mg-0.86Y (wt%, all composition in this paper was in mass percent) by ICP.

Uniaxial tensile experiment specimens were rectangular dog-bone shaped with gauge dimensions of 3 mm×2 mm ×18 mm and tensile axes were parallel to the extruded direction (ED). The tests were carried out in the temperature range of 25 ºC (RT) to 300 ºC and in the strain rate range of 0.001 s^{-1} to 0.1 s^{-1} using MTS (CMT-5105) universal testing machine. For elevated temperature tests, specimens were held on at a specified temperature for 10 min in a furnace equipped in MTS universal testing machine. Each test condition was repeated three times for repeatability.

All microstructure observations were conducted in the plane containing the extrusion direction (ED) and transverse direction (TD). In samples preparation, the mechanical grinding and polishing was used. Then the specimens were etched with a solution of 5 mL HNO_3 and 30 mL H_2O. They were detected by Zeiss Axio Lab A1 optical microscope (OM). Electron Back-Scattered Diffraction (EBSD) data were obtained by Quanta 250FEG emission scanning electron microscope equipped with Oxford Instrument Nordlys Nano EBSD detector. The acceleration voltage was 20 kV and the working distance was 15 mm with a tilt angle of 70°. The EBSD step size of scanning was one-tenth of average grain size for time efficiency and accuracy. The detailed parameter and facilities were the same as the earlier work[6].

2 Results

2.1 Initial microstructure

Fig.1a shows the initial optical microstructure of the extruded Mg-1Y sheet in ED-TD plane. The microstructure consists of α-Mg matrix and a few precipitated phases. The average grain size is (6.2 ± 1.8) μm which was measured by linear intercept method (D = 1.74 L, L was the linear intercept grain size[16]). A few precipitated phases were observed within grains and in grain boundaries. Our previous study[6] has discussed that the precipitated phases were YH_2 phases. Fig.1b reveals inverse pole figure (IPF) map. The white lines and black lines represented low-angle grain boundaries ($2^{\circ} \leqslant \theta < 10^{\circ}$) and high-angle grain boundaries ($\theta \geqslant 10^{\circ}$) in IPF map respectively. Fig.1c shows the grain boundary misorientation angle distribution of the Mg-1Y sheet. Low-angle grain boundaries ratio is 21.0%, corresponding to many low-angle grain boundaries in Fig.1b. Fig.1d shows the {0001} pole figure (PF) of the Mg-1Y sheet. The {0001} PF exhibits a relatively weak basal texture. The maximum intensity is 36.23 MRD and it indicates grains with almost the same orientation. The basal pole deviated into ED with a tendency of spreading in TD, which might be attributed to the non-basal (c+a) slip in extrusion process[17]. Fig.1e shows that inverse pole figure (IPF) for ED. The major intensity distribution is among <11$\bar{2}$2>, <11$\bar{2}$1>, <10$\bar{1}$1>, and <20$\bar{2}$1> and the maximum intensity is 3.57 MRD. The <11$\bar{2}$1> was considered as the "RE texture" component[18] .

2.2 Representative true stress-true strain curves

The representative true stress-true strain curves of the Mg-1Y alloy at the strain rate of 0.01 s^{-1} is illustrated in Fig.2a. After the peak stress, strain softening stages are not remarkable compared with AZ91 and AZ80 under the same deformation condition[19,20]. There are remarkable yield plateaus at the temperature between 150 and 300 ºC. The inapparent flow serration appears in 250 ºC indicating dynamic strain aging (DSA) occurring. The detailed discussion about flow serration is in section 3.1. Fig.2b demonstrates the true stress-true strain of two extreme conditions. Steady flow stage gets longer for strain rate from 0.01 s^{-1} to 0.001 s^{-1} at 300 ºC.

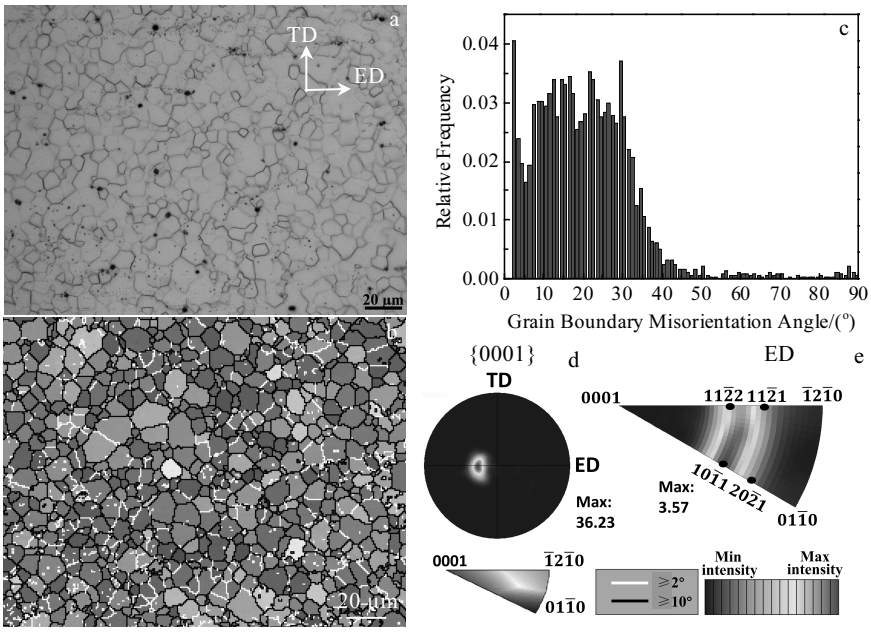

Fig.1 Microstructures of the extruded Mg-1Y sheet: (a) optical micrograph; (b) inverse pole figure map; (c) grain boundary misorientation angle distribution histogram; (d) {0001} pole figure; (e) inverse pole figure for extruded direction (ED)

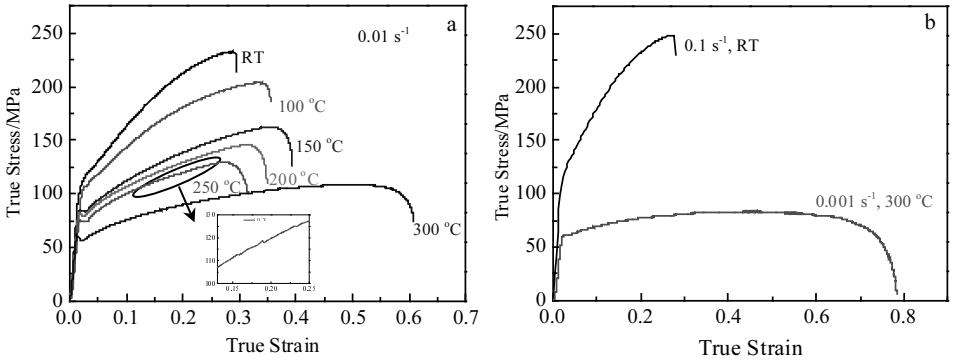

Fig.2 Representative true stress-true strain curves of the alloy at the strain rate of 0.01 s^{-1} (a); tensile true stress-true strain curves of the alloy at two extreme deformation conditions (b)

2.3 Effect of temperature, strain rate on strength and elongation to failure

Fig.3a and Fig.3b demonstrate the effect of temperature and strain rate on ultimate tensile strength (UTS) and yield strength (YS) of the Mg-1Y sheet. UTS and YS decrease with the increase of the temperature and the decrease of strain rate. UTS decreases by 49.3% from (247.9 ± 5.8) MPa to (125.6 ± 4.7) MPa when temperature increases from RT to 300 ºC at the strain rate of 0.1 s^{-1}. Similarly, YS decreases by 32.3% from (106.4 ± 3.2) MPa to (72.0 ± 3.3) MPa under the same condition. The above strength variation indicates that the addition of Y element improved mechanical properties at high temperature. It is interesting to note that the flow behavior of the studied sheet exhibits obvious strain rate sensitivity even at RT. UTS at the strain rate of 0.001 s^{-1} is 88.2% of that at the strain rate of 0.1 s^{-1} at RT. The *m* value is also in favor of it. UTS of the Mg-1Y sheet is lower than that of AZ31 (292.1 MPa)[10] at the strain rate of 0.001 s^{-1} at RT, which may be due to less twinning, weaker solid solution strengthening, and weaker basal texture. The difference of UTS between 0.1 and 0.001 s^{-1} becomes larger in 300 ºC.

Fig.3c illustrates elongation (EL) variation with different tensile temperatures and strain rates. For EL variety, the temperature can be separated into three stages: RT; 100~250 ºC; 300 ºC. EL between 100 and 250 ºC is higher than

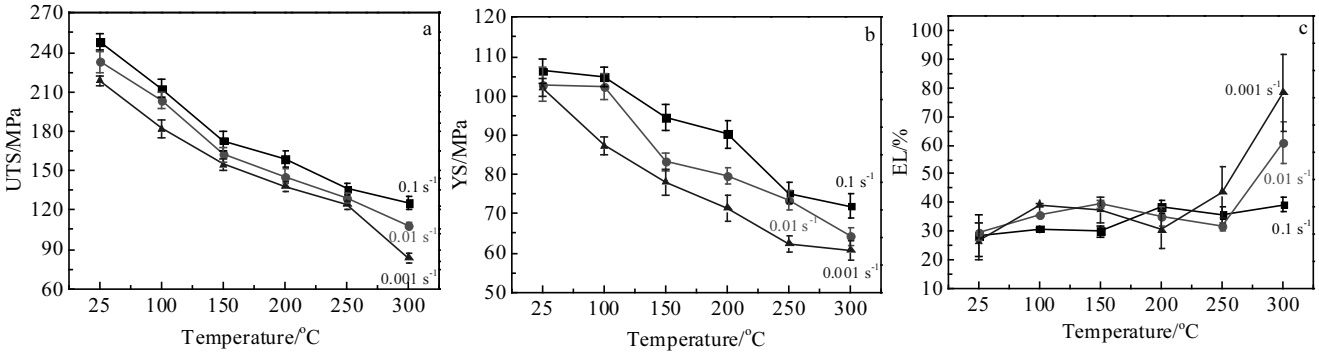

Fig.3 Mechanical properties of the extruded Mg-1Y sheet as a function of tensile temperature at various strain rates: (a) ultimate tensile strength (UTS), (b) yield strength (YS), and (c) elongation to failure (EL)

that at RT. The anomalous EL decrease with the increase of the temperature in specific deformation condition is observed. The temperature ranges for anomalous elongation to failure (EL) reduction increases when strain rate increases: 100~200 ºC at 0.001 s^{-1}, 150~250 ºC at 0.01 s^{-1} and 200~250 ºC at 0.1 s^{-1}. The critical temperature (T_c), at which EL starts to decrease, decreases with the increase of the strain rate. In lower strain rate ranges with lower temperature (0.001 s^{-1} with 100~200 ºC and 0.01 s^{-1} with 150~250 ºC), EL decreases by 12.1% and 10.8%. However at high strain rate with higher temperature (0.1 s^{-1} with 200~250 ºC), EL only decreases by 4.2%. It is the same trend that the critical temperature at which EL started to increase sharply increased with increasing strain rate. EL increases by 293% from RT to 300 ºC at a strain rate of 0.001 s^{-1}, which is due to a larger amount of small grains by DRX. This abnormal EL decrease result will be discussed in section 3.2.

2.4 Constitutive equation

For Mg alloys, the relationship of the peak stress, strain rate, and deformation temperature can be described by the constitutive equation. And the commonly used constitutive equation is the Garofalo hyperbolic sine constitutive equation[14, 21, 22]:

$$\dot{\varepsilon} = A\left[\sinh(\alpha\sigma)\right]^n \exp(-Q/RT) \quad (1)$$

Where $\dot{\varepsilon}$ is strain rate, A and α are material constants, σ is stress, n is exponent of stress, Q is activation energy of deformation, R is universal gas constant, and T is absolute temperature.

The Zener-Hollomon parameter is expressed by[22, 23]:

$$Z = \dot{\varepsilon}\exp\left(\frac{Q}{RT}\right) = A\sinh(\alpha\sigma) \quad (2)$$

Eq.(1) can be evolved by Taylor Series Expansion. Next two equations can be acquired by erasing terms of Taylor Series Expansion at different conditions.

In the condition of the high-stress level ($\alpha\sigma$>1.2), Eq.(3) is obtained approximately.

$$\dot{\varepsilon} = A''\exp(\beta\sigma)\exp(-Q/RT) \quad (3)$$

While in condition of low stress level ($\alpha\sigma$<0.8), Eq.(4) is obtained similarly.

$$\dot{\varepsilon} = A'\sigma^{n'}\exp(-Q/RT) \quad (4)$$

Here A', n', A'', and β are material constants, and $\beta = \alpha n'$.

Eq.(5) and Eq.(6) are derived by Eq.(3) and Eq.(4).

$$1/\beta = (\partial\sigma/\partial\ln\dot{\varepsilon})_T \quad (5)$$

$$1/n' = (\partial\ln\sigma/\partial\ln\dot{\varepsilon})_T \quad (6)$$

UTS was used in this work for the fitting. The linear fitting of σ-ln$\dot{\varepsilon}$ and lnσ-ln$\dot{\varepsilon}$ are illustrated in Fig.4.

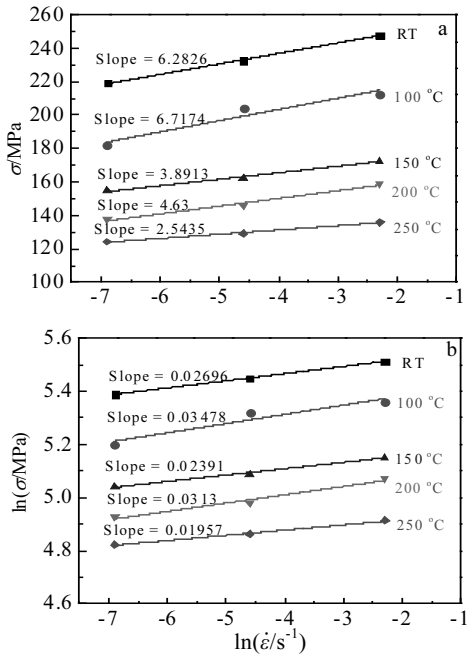

Fig.4 Relationship of σ-ln$\dot{\varepsilon}$ (a) and lnσ-ln$\dot{\varepsilon}$ (b)

By calculating the average slope value of two stress condition in Fig.4, $1/\beta$ and $1/n'$ are obtained. So $\alpha = \beta/n' = 0.00567$ mm^2/N.

From Eq.(1), Eq.(7) and Eq.(8) were obtained.

$$1/n = \{\partial[\ln\sinh(\alpha\sigma)]/\partial\ln\dot{\varepsilon}\}_T \quad (7)$$

$$Q = nR\{\partial[\ln\sinh(\alpha\sigma)]/\partial(1/T)\}_\varepsilon \quad (8)$$

Similarly, n and Q can be calculated by Fig.5. The value of n is 27.8, and Q is 124.6 kJ/mol.

From Eq.(2),

$$\ln Z = \ln A + \ln\sinh(\alpha\sigma) \quad (9)$$

So, $\ln A$ is the Y-intercept of Fig.6 (29.13). A is 4.48×10^{12}. The constitutive equation was determined as Eq.(10).

$$\dot{\varepsilon} = 4.48\times10^{12}[\sinh(0.00567\alpha)]^{27.8}\exp(-\frac{124600}{RT}) \quad (10)$$

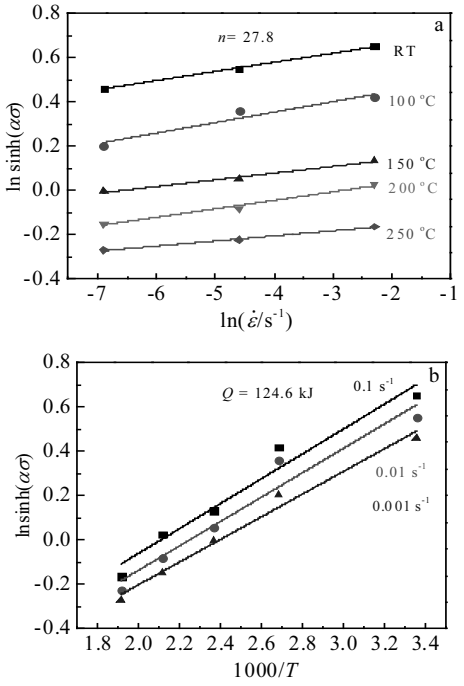

Fig.5 Relationship of $\ln\sinh(\alpha\sigma)$ - $\ln\dot{\varepsilon}$ (a) and $\ln\sinh(\alpha\sigma)$ - $1000/T$ (b)

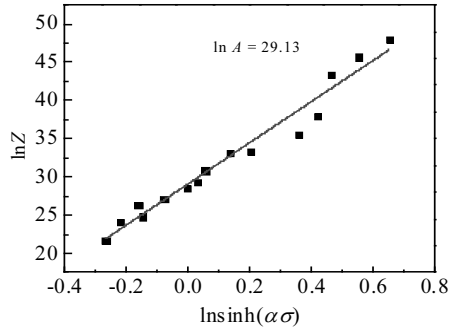

Fig.6 Relationship of $\ln Z$ - $\ln\sinh(\alpha\sigma)$

The experimental values and calculated values are summarized in Table 1. The average error is 2.8%, calculated by Eq.(11):

Average error=

$$\frac{1}{N}\sum_i^N[|\frac{\text{Measured stress} - \text{Predicated stress}}{\text{Measured stress}}|]\times100\% \quad (11)$$

2.5 Strain rate sensitivity

Strain rate sensitivity is an important parameter to interpret the plastic deformation. Strain rate sensitivity indicated the different true stress for different strain rates [24, 25], represented by Eq.(12):

$$m = \frac{\partial\ln\sigma}{\partial\ln\dot{\varepsilon}} \quad (12)$$

Where m is strain rate sensitivity value.

Fig.7a, Fig.8a, Fig.9a illustrate the true stress-true strain flows for different strain rates at RT, 200, 300 ºC, respectively. The influence of strain rate on flow increases with the increase of the temperature. At RT, UTS decreases by 11.8% with the strain rate decreasing from 0.1 s^{-1} to 0.001 s^{-1}. This indicates that the effect of strain rate on flow characteristic is obvious with m=0.022~0.027, which is not consistent with AZ31[10]. Li et al[26] found that strain rate had an anomalous positive dependence of elongation in Mg-Gd-Y alloy at RT, which was contributed to activation of non-basal slip system. Xu et al[27] found that the same

Table 1 Comparison of experimental UTS value and calculated UTS value by constitutive equation for all conditions

Temperature/ ºC	Strain rate/ s^{-1}	Experimental value/MPa	Calculated value/MPa	Error/ %
25	0.1	247.9	252.4	1.8
	0.01	232.6	239.5	3.0
	0.001	219.0	226.8	3.6
100	0.1	212.7	197.7	7.1
	0.01	203.7	186.0	8.7
	0.001	181.8	174.8	3.9
150	0.1	172.7	174.1	0.8
	0.01	162.3	163.2	0.6
	0.001	154.8	152.8	1.3
200	0.1	159.0	156.6	1.5
	0.01	145.7	146.5	0.5
	0.001	137.7	136.8	0.7
250	0.1	136.0	143.4	5.4
	0.01	129.3	133.8	3.5
	0.001	124.3	124.7	0.3

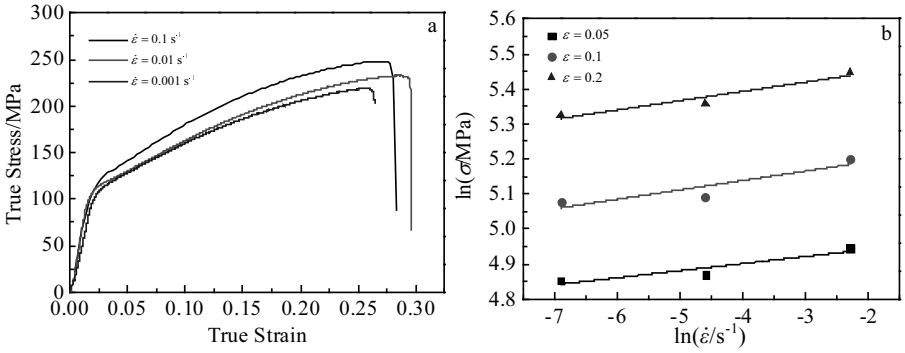

Fig.7 True stress-true strain curves of Mg-1Y sheet tensile at strain rates of 0.1, 0.01 and 0.001 s^{-1} at 25 ºC (a); relationship of $\ln\sigma$ - $\ln\dot{\varepsilon}$ to determine *m* value at strains of 0.05, 0.1 and 0.2 at 25 ºC (b)

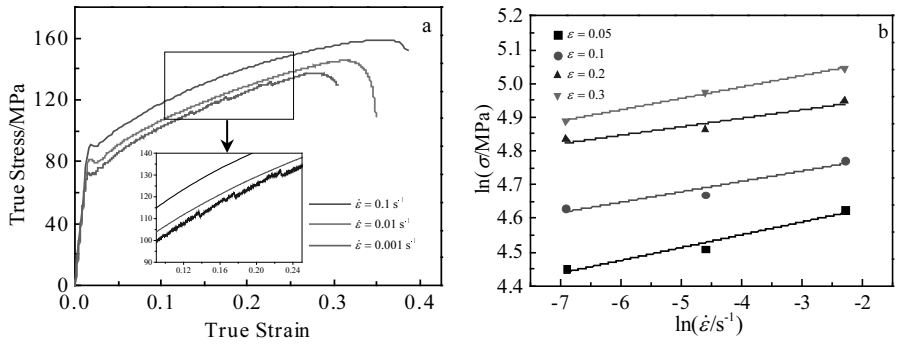

Fig.8 True stress-true strain curves of Mg-1Y sheet tensile at strain rates of 0.1, 0.01 and 0.001 s^{-1} at 200 ºC (a); relationship of $\ln\sigma$ - $\ln\dot{\varepsilon}$ to determine *m* value at strains of 0.05, 0.1 and 0.2 at 200 ºC (b)

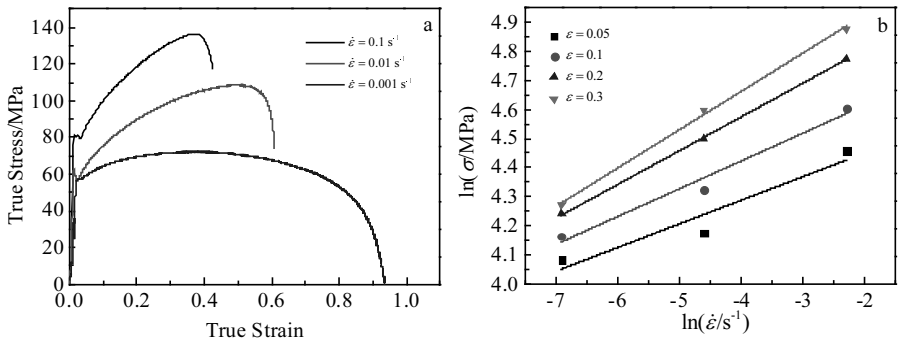

Fig.9 True stress-true strain curves of Mg-1Y sheet tensile at strain rates of 0.1, 0.01 and 0.001 s^{-1} at 300 ºC (a); relationship of $\ln\sigma$ - $\ln\dot{\varepsilon}$ to determine *m* value at strains of 0.05, 0.1, 0.2 and 0.3 at 300 ºC (b)

trend in Mo-Re alloy at RT. Flow serration appeared at the strain rate of 0.001 s^{-1} in 200 ºC. At relatively high temperature, yield plateau was observed which were related to dislocation pin-in and pin-off.

Fig.7b, Fig.8b, Fig.9b show $\ln\sigma$ versus $\ln\dot{\varepsilon}$ at the different true strains. The linear fitting results are also displayed. The strain rate sensitivity *m* which is calculated by the slope of fitting lines by Eq.(12), are summarized in Table 2. The *m* value increases as the increase of the temperature. And the same tendency is followed by the effect of different strains at RT and 300 ºC. It is worthwhile to notice that *m* decreases from the strain of 0.05 to 0.2 at 200 ºC firstly, and then increases until the strain of 0.3.

2.6 Deformation microstructure

Fig.10 shows the optical micrographs of deformation microstructure at the strain rates of 0.1 and 0.001 s^{-1} with

the temperatures of RT, 200, 300 ºC. More in quantity twins appear at RT and a few twins appeared at 200 ºC. Twinning was restrained as the temperature increased and disappeared at 300 ºC. Several obvious twins were labeled by white arrows in Fig. 10. Grains were elongated at 200 and 300 ºC. Due to sufficient nucleation time[28] and temperature, DRX occurred at 0.001 s^{-1}, 300 ºC. Smaller grains by DRX have an influence in higher *m* value [29, 30].

3 Discussion

3.1 Flow serration

Fig.2a and Fig.8a show that flow serrations appear in the strain rate of 0.01 s^{-1} at 250 ºC, and in the strain rate of 0.001 s^{-1} at 200 ºC.

Flow serration was reported in many Mg alloys and related to dynamic strain aging (DSA) by many researchers[31-35]. DSA indicated that deformation behavior was controlled by slip movement, which resulted from the interaction between solute atoms and moving dislocations [34]. Gao et al[35]found Mg-Y binary alloys presenting serrated flow in temperature of 150 ºC to 250 ºC, in which the dislocation and solute Y atoms have interaction. The similar temperature range (150 ºC to 225 ºC) was obtained for flow serration in WE54 and other Mg alloys[31-35]. In view of similar temperature range and strain rate range, flow serration in this study may be related to DSA.

On the other hand, the flow serration is also related to the shearing of precipitated by dislocation[32]. In the present study, Fig.1a and Fig.10 demonstrate that the precipitated phase exists. The effect of precipitate on flow serration should not be ignored. Further investigation needs to corroborate the effect of precipitates on flow serration.

Flow serrations are only observed at 200 and 250 ºC and in the strain rates of 0.01 and 0.001 s^{-1}. Elevated temperature improves slip movement velocity in Mg alloys. Meanwhile lower strain rate implied that more time was taken to form dislocation pile-up[36]. So they are perhaps the reasons why flow serrations were only observed at a relatively higher temperature and in the strain rates of 0.01 and 0.001 s^{-1}.

3.2 Anomalous EL decrease

Fig.3c illustrates EL variation with different tensile temperatures and strain rates. The anomalous EL decreases with the increase of the temperature in specific deformation condition, including temperature ranges of 100 to 200 ºC at the strain rate of 0.001 s^{-1}, 150 to 250 ºC at the strain rate of 0.01 s^{-1} and 200 to 250 ºC at the strain rate of 0.1 s^{-1}. The critical temperature (T_c) at which EL starts to decrease increases with the increase of the strain rate.

Table 2 Strain rate sensitivity values (*m*) calculated by Fig.7b, Fig.8b and Fig.9b at different temperatures and strains

Temperature/ºC	Strain			
	0.05	0.1	0.2	0.3
25	0.022	0.026	0.027	-
200	0.038	0.031	0.025	0.034
300	0.068	0.079	0.094	0.110

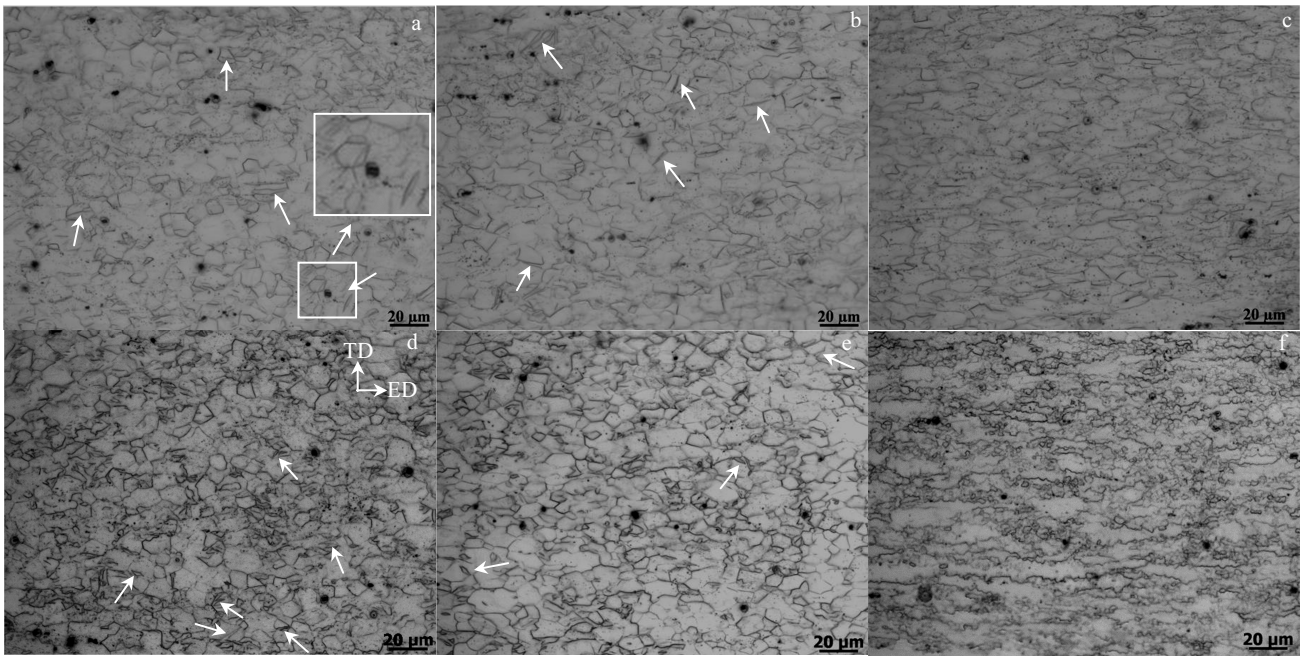

Fig.10 Optical microstructures of the Mg-1Y sheet tensile to fracture at different conditions: (a) RT, 0.1 s^{-1}; (b) 200 ºC, 0.1 s^{-1}; (c) 300 ºC, 0.1 s^{-1}; (d) RT, 0.001 s^{-1}; (e) 200 ºC, 0.001 s^{-1}; (f) 300 ºC, 0.001 s^{-1}

When tensile temperature is up from 100 to 200 ºC at 0.001 s^{-1}, EL decreases by 12.1% from 47.6%, where DSA takes place (flow serration in 200 ºC). Similarly, when tensile temperature is up from 150 ºC to 250 ºC at 0.01 s^{-1}, EL decreases by 10.8% from 48.2%, in which DSA appears (flow serration in 250 ºC). While tensile temperature is up from 200 ºC to 250 ºC at 0.1 s^{-1}, EL decreases only by 4.2% from 47.0%. No flow serration appears in true stress-true strain curves.

EL increasing with the increase of the temperature have been observed by many researchers[14,37]. When temperature increased, the strain hardening region was narrowed and steady flow region was enlarged[38]. For Al alloys[39-41] and Mg alloys[2, 33], the presence of serration was related to a decrease of ductility. Stanford et al.[2] and Robinson et al.[42] reported negative SRS can reduce the ductility. Negative SRS was usually related to DSA for strain rate jump test. So it is reasonable to believe that DSA plays a huge contribution to the decrease of EL in present research because of the temperature range anastomose. In addition, the activation of the dynamic recovery process also results in lower EL [2]. Dynamic recovery should not be ignored in spite of no observation in this work.

The critical temperatures at which ELs start to increase sharply increase as strain rates rise. When temperature rises to 300 ºC, EL increases rapidly except for that in 0.1 s^{-1}. In Fig. 10, DRX occurred in the strain rate of 0.001 s^{-1} at 300 ºC and many small grains nucleated and grew in grain boundaries. However, in the strain rate of 0.1 s^{-1} at 300 ºC, grains are only elongated and few small grains are found. Through DRX, deformation can be dispersed into a large number of grains by the formation of small grains. Small grains can play a significant role in deformation to improve EL.

3.3 Constitutive equation

For the present result, the stress exponent n is 27.8, and activity energy Q is 124.6 kJ/mol in the strain rate range of 0.001 to 0.1 s^{-1} with temperature from RT to 250 ºC. The attempt of establishing a constitutive equation in the temperature range of RT to 300 ºC had been done. The all fitting slopes of 300 ºC are far from that of RT to 250 ºC and the error is 14%. Many previous researchers[43, 44] investigated different constitutive equation during different temperature regions. Chen et al[43] interviewed the Al alloy 7075 and found that two different constitutive equations corresponding to different microstructure. For Al alloy 7075, the constitutive behavior in the wide temperature range (350 ºC to 600 ºC) can be divided into two types: plastic deformation when the alloy is in solid state and containing a small fraction of liquid (350 ºC to 490 ºC); thixotropic deformation when the alloy in the semi-solid state (above 490 ºC). Our previous study[6] observed inconspicuous grain growth in 300 ºC annealing for the Mg-1Y sheet. Grain growing and hardness decreasing were observed in 350 ºC annealing for extruded Mg-1Y bar[45]. Fig. 10 shows small grains evolved by DRX at 300 ºC and no DRX under 300 ºC. This gives us sufficient reasons to doubt that microstructure changing lead to fitting failure of 300 ºC.

The stress exponent is 27.8, which is higher than the previous interview. The reason for high n value is not clear yet. But some researchers believe that second phase particles could lead to high-stress exponent[46, 47]. Fig. 1a and Fig. 10 illustrate the second phase exits in the studied material. Activity energy is 124.6 kJ/mol, which is close to self-diffusion in Mg, indicating deformation mechanism was controlled by dislocation climb.

3.4 Strain rate sensitivity

Table 2 shows strain rate sensitivity m with variant temperatures and strains. All m values are small and less than 0.11. The m value increases with the increase of the temperature. Karimi et al[24] researched the effect of temperature on deformation in AZ31 and the SRS value (m value) can be derived as Eq.(13):

$$m = \frac{\partial \ln \sigma}{\partial \ln \dot{\varepsilon}} = \frac{\partial \ln \sigma_{\text{th}}}{\partial \ln \dot{\varepsilon}} = \left(\frac{\partial \sigma_{\text{th}}}{\partial Q}\right)\left(\frac{\partial Q}{\partial \ln \dot{\varepsilon}}\right) = \frac{kT}{V} \tag{13}$$

Where σ_{th} is the thermal activation stress, other symbol have been referred to before. This equation indicates the strong dependence of m value to deformation temperature and m value increases with the increase of the temperature.

The effect of temperature means the change of deformation mechanism from twin-dominant to dislocation slip-dominant. Fig.10 illustrates that with deformation temperature increasing, twinned area fraction becomes smaller. At 300 ºC no twins appeared and DRX took place. The twin was found to influence SRS at a lower temperature in AZ31[24]. For lack of independent slip systems, twinning plays an important role to accommodate the strain at a relatively low temperature. As temperature increases, the CRSS for slip systems decreases and more slip systems are activated[48]. Therefore, the contribution of dislocation slip took the lead relatively, accompanying DRX in relatively high temperature. At 300 ºC, m value increasing with strain implies the dislocation slip as the dominant deformation mechanism in AZ31[49]. In another AZ31 study[24], there is no variant m value in 300 ºC at the different strain. This indicated no more slip system was activated except for prismatic <*a*> slip in AZ31 in the same condition. Therefore the addition of Y can improve the deformation ability of Mg alloys by activation of more slip systems.

Generally, m value increases with strain because dislocation multiplied during deformation. It is worthwhile to notice that m value decreases from 0.038 to 0.025 for the strain from 0.05 to 0.2 at 200 ºC. Firstly twins have an influence on SRS in previous studies. The increased twinning

activity in AZ91 is related to lower SRS. Chun et al[50] reported lower SRS in highly textured wrought AZ31 sheets indicating inducing twin would reduce SRS. On the other hand, the DSA occurred at 200 ºC from 0.1 to 0.2 in Fig.8a. When DSA takes place, dislocation movement is restricted by solute and slip becomes more difficult. Meanwhile, twin is easy to activate and plays an important role in deformation. Therefore the *m* value reduction from 0.038 to 0.025 for the strain from 0.05 to 0.2 in 200 ºC might be attributed to twinning and DSA.

4 Conclusions

1) Increasing temperature and decreasing strain rate result in decreasing UTS and YS. The Mg-1Y sheet exhibits obvious strain rate sensitivity even at RT. The UTS at RT decreases by 11.8% as the strain rate decreases from 0.1 s^{-1} to 0.001 s^{-1}.

2) The anomalous EL reduction occurs at intermediate temperature range. Flow serration appears in the strain rate of 0.01 s^{-1} at 250 ºC, and in the strain rate of 0.001 s^{-1} at 200 ºC. The anomalous EL reduction and flow serration are believed to be closely related to DSA.

3) The constitutive equation in the temperature range of RT to 250 ºC, the strain rate range of 0.001 s^{-1} to 0.1 s^{-1}:

$$\dot{\varepsilon} = 4.48\times10^{12}\,[\sinh(0.00567\alpha)]^{27.8}\exp(-\frac{124600}{RT})$$

And deformation is controlled by dislocation climb.

4) The *m* value increases with the increase of the temperature. The maximum *m* value is 0.11 in the strain of 0.3 at 300 ºC, indicating the addition of Y results in the activition of more slip systems.

5) Twinning is depressed with temperature and disappears until 300 ºC. At 300 ºC, dynamic recrystallization is observed, and it is promoted by lower strain rate.

References

1 Kulekci M K. *International Journal of Advanced Manufacturing Technology*[J], 2008, 39(9-10): 851

2 Stanford N, Sabirov I, Sha G *et al. Metallurgical and Materials Transactions A*[J], 2010, 41(3): 734

3 Hamad K, Ko Y G. *Scientific Reports*[J], 2016, 6(1): 29 954

4 Ren L B, Quan G F, Xu Y G *et al. Journal of Alloys and Compounds*[J], 2017, 699: 976

5 Borkar H, Pekguleryuz M. *Metallurgical and Materials Transactions A*[J], 2015, 46(1): 488

6 Huang G H, Yin D D, Lu J W *et al*. *Materials Science and Engineering A*[J], 2018, 720: 24

7 Abbasi-Bani A, Zarei-Hanzaki A, Pishbin M H *et al*. *Mechanics of Materials*[J], 2014, 71: 52

8 Wang H, Boehlert C J, Wang Q D *et al*. *Materials Characterization*[J], 2016, 116: 8

9 Máthis K, Trojanová Z, Lukáč P. *Materials Science & Engineering A*[J], 2002, 324(1): 141

10 Maksoud I A, Ahmed H, Rödel J. *Materials Science and Engineering A*[J], 2009, 504(1-2): 40

11 Ren L, Wu J, Quan G. *Materials Science and Engineering A* [J], 2014, 612: 278

12 Zhang L, Jia R, Li D *et al*. *Journal of Materials Science & Technology*[J], 2015, 31(5): 504

13 Wu G, Fan Y, Gao H *et al*. *Materials Science and Engineering A*[J], 2005, 408(1-2): 255

14 Lu J W, Yin D D, Ren L B *et al*. *Journal of Materials Science*[J], 2016, 51(23): 10 464

15 Stanford N, Barnett M R. *Materials Science and Engineering A*[J], 2008, 496(1-2): 399

16 Korla R, Chokshi A H. *Metallurgical and Materials Transactions A*[J], 2014, 45(2): 698

17 Agnew S R, Yoo M H, Tomé C N. *Acta Materialia*[J], 2001, 49(20): 4277

18 Huppmann M, Gall S, Müller S *et al*. *Materials Science and Engineering A*[J], 2010, 528(1): 342

19 Cai Y, Wan L, Guo Z H *et al*. *Materials Science and Engineering A*[J], 2017, 687: 113

20 Wei Y H, Wang Q D, Zhu Y P *et al*. *Materials Science and Engineering A*[J], 2003, 360(1-2): 107

21 Mirzadeh H. *Mechanics of Materials*[J], 2014, 77: 80

22 Evangelista E, Spigarelli S. *Metallurgical & Materials Transactions A*[J], 2002, 33(2): 373

23 Park S H, Kim H S, You B S. *Metals and Materials International*[J], 2014, 20(2): 291

24 Karimi E, Zarei-Hanzaki A, Pishbin M H *et al*. *Materials & Design*[J], 2013, 49(4): 173

25 Lee W, Chen T. *Scripta Materialia*[J], 2006, 54(8): 1463

26 Li J L W D C R. *Acta Materialia*[J], 2018, 159: 31

27 Xu J, Leonhardt T, Farrell J *et al*. *Materials Science & Engineering A*[J], 2008, 479(1): 76

28 Jin X, Xu W, Shan D *et al. Metals and Materials International*[J], 2017, 23(3): 434

29 Wang H, Xue E, Nan X *et al*. *Scripta Materialia*[J], 2013, 68(5): 229

30 Del Valle J A, Ruano O A. *Scripta Materialia*[J], 2006, 55(9): 775

31 Trojanová Z, Lukáč P, Milička K *et al*. *Materials Science and Engineering A*[J], 2004, 387-389: 80

32 Wang C, Xu Y, Han E. *Materials Letters*[J], 2006, 60(24): 2941

33 Zhu S M, Nie J F. *Scripta Materialia*[J], 2004, 50(1): 51

34 Corby C, Cáceres C H, Lukáč P. *Materials Science and Engineering A*[J], 2004, 387-389: 22

35 Gao L, Chen R S, Han E H. *Journal of Alloys and Compounds*[J], 2009, 472(1-2): 234

36 Wang W H, Di W U, Chen R S *et al*. *Transactions of Nonferrous Metals Society of China*[J], 2015, 25(11): 3611

37 Agnew S R, Duygulu Ö. *International Journal of Plasticity*[J], 2005, 21(6): 1161

38 Mulford R A, K. *Acta Metallurgica*[J], 1979, 27(7): 1125

39 Bouchaud E, Kubin L, Octor H. *Metallurgical Transactions A*[J], 1991, 22(5): 1021
40 Saha G G, Mccormick P G, Rao P R. *Materials Science & Engineering A*[J], 1984, 62(2): 187
41 Pink E K J. *Materials Science & Engineering A*[J], 1985, 1-2(75): 87
42 Robinson J M, Shaw M P. *Metallurgical Reviews*[J], 1994, 39(3): 113
43 Chen G, Lin F, Yao S *et al*. *Journal of Alloys and Compounds*[J], 2016, 674: 26
44 Galiyev A S O K R. *Materials Transactions*[J], 2003, 44(4): 426
45 Wei J, Huang G, Yin D *et al*. *Metals*[J], 2017, 7(4):119
46 Yin D D, Wang Q D, Janik V. *Metallurgical & Materials Transactions A*[J], 2012, 43(9): 3338
47 Barnett M R, Keshavarz Z, Beer A G *et al*. *Acta Materialia*[J], 2004, 52(17): 5093
48 Srinivasarao B, Dudamell N V, Pérez-Prado M T. *Materials Characterization*[J], 2013, 75: 101
49 Korla R, Chokshi A H. *Scripta Materialia*[J], 2010, 63(9): 913
50 Chun Y B, Davies C H J. *Materials Science and Engineering A*[J], 2011, 528(18): 5713

应变速率和温度对 Mg-1Y 挤压板材拉伸变形行为的影响

纪　彬[1]，陆嘉伟[1]，于逸翔[2]，尹冬弟[1]
(1. 西南交通大学 材料先进技术教育部重点实验室，四川 成都 610031)
(2. 江苏朗顺电工电气有限公司，江苏 扬州 225800)

摘　要：在温度为 25~300 ℃ 应变速率为 0.001~0.1 s^{-1} 的范围内研究了 Mg-1Y (质量分数，%) 挤压板材的拉伸变形行为。结果表明：在 0.1 s^{-1} 的应变速率下，当温度从室温增加至 300 ℃时抗拉强度从(247.9±5.8) MPa 到(125.6+4.7) MPa 降低了 49.3%。板材即使在室温下也表现出了明显的应变速率敏感性。室温下，当应变速率从 0.1 s^{-1} 降低至 0.001 s^{-1}，抗拉强度降低 11.8%。在室温和 250 ℃温度范围内可以通过 Garofalo 双曲正弦本构方程来描述合金的流变行为。测得的应力指数 n 为 27.8±8.9，激活能 Q 为(124.6±6.1) kJ/mol，Q 值意味着变形是位错攀移控制。在中间温度（150~250 ℃）时板材表现出锯齿流变行为，这种现象在较低应变速率更明显。同时断裂延伸率随着温度升高而反常地降低。认为上述 2 种变形特征和 Y 原子和位错的强烈的相互作用有关系，这种作用即为动态应变时效（DSA）。应变速率敏感因子（m）随温度升高而增加。在 300 ℃下 m 从 0.068 增加至 0.11，说明 Y 元素的添加可以激活更多滑移系。变形后显微组织的观察表明孪晶被温度抑制，同时与增大的 m 相一致。300 ℃下观察到有动态再结晶（DRX）的出现，应变速率越低 DRX 越明显。

关键词：Mg-1Y挤压板材；拉伸变形；本构方程；应变速率敏感因子

作者简介：纪 彬，男，1993 年生，硕士，西南交通大学材料科学与工程学院，四川 成都 610031，电话：028-87634673，E-mail: 1625225064@qq.com